Plane-wave theory of three-dimensional magnonic crystals

M. Krawczyk and H. Puszkarski
Surface Physics Division, Faculty of Physics, Adam Mickiewicz University, Umultowska 85, Poznań 61-614, Poland
(Received 3 September 2007; revised manuscript received 5 November 2007; published 27 February 2008)

We use the plane-wave method to determine spin-wave spectra of three-dimensional magnonic crystals (the magnetic counterpart of photonic crystals) composed of two different ferromagnetic materials. The scattering centers in the magnonic crystal considered are ferromagnetic spheroids (spheres being a special case) distributed in sites of a cubic (sc, fcc, or bcc) lattice embedded in a matrix of a different ferromagnetic material. We demonstrate that magnonic gaps in such structures occur at spontaneous magnetization contrast and/or exchange contrast values above a certain critical level, which depends on the lattice type. Optimum conditions for magnonic gaps to open are offered by the structure in which the scattering centers are the most densely packed (the fcc lattice). We show that in all three lattice types considered the reduced width of the gap (i.e., the width referred to the gap center) is, in good approximation, a linear function of both the exchange contrast and the magnetization contrast. Also, the gap width proves sensitive to scattering center deformation, and its maximum value to correspond to a scattering center shape close to a sphere. Moreover, our numerical results seem to indicate that dipolar interactions in general result in an effective reduction of the gap width, but their impact only becomes of importance when the lattice constant of the cubic magnonic structure is greater than the ferromagnetic exchange length of the matrix material.

DOI: 10.1103/PhysRevB.77.054437 PACS number(s): 75.30.Ds, 75.70.Cn, 75.40.Gb

I. INTRODUCTION

The currently available techniques of microstructure and nanostructure fabrication allow us to design materials of physical properties not found in naturally formed substances. Such structures include, among others, metamaterials with negative effective permittivity and permeability,[1–3] metamaterials with zero effective permittivity,[4,5] or dielectric composite materials in which the velocity of electromagnetic wave propagation can be widely controlled;[6–8] also some phononic crystals are unusual media for elastic waves.[9–12] Few papers have been published so far on *magnonic* crystals, which are the *magnetic* counterpart of photonic crystals, with spin waves acting as information carriers. Also these composite materials open the pathway to production of materials with properties not found in homogeneous structures. In this study we investigate the spin dynamics in magnonic composite materials by scrutinizing the dispersion of spin waves, the propagation of which is the basis of many physical effects occurring in magnetic nanostructures (e.g., spin switching and magnetization reversal,[13–15] or spin current[16,17]).

The determination of the spin-wave dispersion in homogeneous ferromagnetic materials is a well-studied problem widely discussed in the literature (see, e.g., Refs. 18 and 19). In finite structures the spin-wave spectrum substantially depends on the surface conditions (usually expressed by surface anisotropy;[20,21]) uncompensated magnetic dipoles on the ferromagnet surface should be taken into account as well, as they result in a static demagnetizing field which is nonhomogeneous in the bulk and generally can be calculated numerically.[22,23] Only in ellipsoidal structures the demagnetizing field is homogeneous and can be determined analytically. Let us add that besides the static component of the demagnetizing field, also the dynamic one, stemming from the dynamic component of the magnetization vector, has an impact on the spin-wave spectrum.

In nonhomogeneous magnetic materials extra factors are added to contribute to the dispersion relation; the most important of them is the magnetic nonhomogeneity. In a composite made from different magnetic materials the internal nonhomogeneity is a consequence of different values of magnetic parameters in the constituent materials. Also in homogeneous materials, under certain external (thermodynamic) conditions, spontaneous separation of magnetic phases may occur, resulting in the formation of regions of different magnetic properties. Another example of nonhomogeneous magnetic structure is a system of magnetic domains, with uniformly magnetized regions (separated by domain walls) of different orientation of the magnetization vector. An interesting situation occurs when the magnetic nonhomogeneity is *only* due to a nonhomogeneity of the magnetic field (internal or external).

The character of a spin-wave spectrum is also known to substantially depend on the type of interactions (dipolar or exchange) prevailing in the system.[24] The most common criterion in determining which interactions predominate is the spin-wave length (the wave vector) and, in the case of finite materials, the ratio of the sample size to the material parameter referred to as the exchange length.[19] If the dipolar interactions prevail, the so-called magnetostatic approximation, in which the effect of exchange interactions is assumed to be negligible, can be used; and vice versa, in the case of exchange interaction predomination, the effect of dipolar interactions can be neglected in calculations.[25] In the transition (dipolar-exchange) range both types of interactions are of importance and must be taken into account. In one of our earlier papers[24] we have shown that the nonhomogeneous internal magnetic field resulting from the predominance of dipolar interactions renders the spin-wave spectrum very complex even in homogeneously magnetized ferromagnetic materials.

In this study we consider model situations in which the nonhomogeneity in a magnetic material is *periodic* in space;

effects not observed in homogeneous materials can be expected to occur in such structures. This expectation is well founded, since such periodic magnetic composite materials can be regarded as the magnetic counterpart of photonic or phononic crystals, with spin waves (rather than electromagnetic or elastic ones) acting as information carriers. The fundamental feature of periodic magnetic structures [referred to as magnonic crystals (MCs)] is an energy gap in their spectrum of magnetic excitations; the gap represents a range of energy values in which spin-wave excitations are forbidden from propagating. Depending on the dimensionality of the space in which the structure is periodic, magnonic structures are one dimensional (1D), two dimensional (2D), or three dimensional (3D).[26–42]

The simplest examples of 1D magnonic crystals are multilayers and magnetic superlattices composed of alternating layers of different magnetic materials, or of magnetic and nonmagnetic ones.[43–46] Magnonic gaps (MGs) in these materials only occur in the spectrum of spin waves propagating in the direction perpendicular to the layer plane. Despite their structural simplicity, 1D MCs abound in effects specific to periodic composite materials. When sublayers of a magnetic material alternate with those of a nonmagnetic metallic material, the coupling between sublayers is based on electron interaction (the Ruderman-Kittel-Kasuya-Yosida interaction), and oscillates with increasing thickness of the nonmagnetic sublayer; as a consequence, the coupling can be either ferromagnetic or antiferromagnetic. A simplified model, with the metallic interlayer replaced by the exchange integral J_{eff} which is the measure of coupling between adjacent ferromagnetic sublayers, can be used for description of spin waves in such a system, which in this approach formally becomes a multilayer composed of directly adjoining ferromagnetic layers. This method requires a careful description of the conditions on the interfaces.[47]

Another example of 1D MC is a "strip" domain system, composed of alternating magnetic strips in which the magnetization vector is oriented in opposite directions; such systems can be regarded as superlattices of finite thickness. Spin waves propagating in such a system[48–51] have a very complex dispersion relation, as the transfer of excitation energy between domains is significantly affected by the domain walls, which have their own dynamics.[52] The picture becomes even more complex in systems of double periodic structure, which include multilayer systems composed of strip sublayers[53] (the double periodicity results from combining the periodicity of strips within the layer plane with that of sublayers made of different materials). Also comblike structures and serial loop structures, in which a magnonic energy gap was found to exist, can be regarded as 1D magnonic crystals.[54–56]

Pioneered by Vasseur *et al.*[57] a decade ago, the theory of 2D MCs has been since developed by several research groups.[58–60] The recently performed first experiments on 2D MCs[61] were aimed at studying the processes of magnetization[62,63] and magnetostatic wave transmission;[64] in these structures; the periodic composite materials used in these studies had been fabricated by drilling regularly distributed holes in a ferromagnetic material. Two-dimensional MCs can also be realized by systems of ferromagnetic rods forming a 2D crystallographic lattice and embedded in a magnetic or nonmagnetic matrix, or by a periodic antidot structure formed in a magnetic material.[65–69] The properties of a 2D MC spin-wave spectrum depend on a number of factors. In an MC composed of two different magnetic materials that form a periodic structure with lattice constant in the order of tens to hundreds of nanometers, exchange interactions (both within and between the constituent materials) are predominant, but the significance of dipolar interactions grows as the lattice constant of the magnonic structure increases. The situation is similar in MCs composed of a ferromagnet and a nonmagnetic prevails in such structures due to the absence of the exchange coupling between the rods (whereas exchange spin waves prevail within the rods when the lateral dimensions of the latter are comparable to the exchange length). In the three coupling ranges: the exchange, the dipolar exchange, and the magnetostatic ones, spin waves in an MC show qualitatively different dispersions. The recently published studies of ferromagnetic layers with periodically modulated surface take the challenge in this context. Nikitov *et al.*,[70] in a study of an yttrium iron garnet (YIG) layer of $5-16$ μm thickness with a lattice of holes drilled in the surface to the depth of $1-2$ μm, found that the surface periodicity has an impact on the spectrum of magnetostatic waves and on the MG opening.

A distinct group of composite materials, magnetophotonic crystals (MPCs), or photonic crystals made from magnetic constituent materials, offers the possibility of modulating some of their optical properties by controlling the applied magnetic field. This opens the door to new applications;[71,72] an interesting effect of possible practical use is the electromagnetic unidirectionality (described by Figotin and Vitebsky[73,74]) in structures with asymmetric dispersion relation. Equally interesting is the possibility of occurrence of the so-called giant photonic Hall effect, in which the refraction angle of an electromagnetic wave in an MPC depends on both the wave polarization and the applied magnetic field.[75] Measurements of electromagnetic wave transmission through a superlattice comprising a 2D magnetic composite as a constituent material are reported in Refs. 76–78; a magnetophotonic gap is demonstrated to open as a result of ferromagnetic resonance of a frequency in the vicinity of the gap.[77,78] Two-dimensional magnetophotonic crystals can be realized by distributing ferromagnetic rods or drilling holes in a magnetic matrix (with lattice constant up to 100 nm).[79]

Magnetophotonic crystals open the pathway to interesting practical applications based on the effect of magneto-optical coupling. Of principal use is the coupling between electromagnetic and magnetostatic waves, due to the broad frequency range (extending up to the order of gigahertz) of the latter. Magnetostatic waves allow us to anticipate devices based on such magneto-optical coupling to replace those operating in the rf range and using acoustic surface waves. Besides this, other possible applications of periodic composites in the form of MCs,[80] and even of materials with just periodically modulated surface,[81,82] are described in the literature.

An important factor determining the magnonic spectrum (in particular, the width of the energy gaps) is the interface between the constituent materials of the composite. Also the

intermediate layer that forms in this zone of diffusion of atoms of the adjacent layers of different materials[83] has its contribution to the conditions of energy gap opening. This problem has been quite thoroughly studied in the case of 1D magnetic superlattices;[84–86] "smoothening" of the magnetic interface and modification of its thickness have been shown to substantially affect the width of the magnonic gap (in 1D crystals the interface is modeled by parameter modulation described by trigonometric[84] or elliptic[85] functions). However, the dependence of the spin-wave spectrum on the interface "quality" in 2D and 3D MCs has not yet been analyzed in detail.

A survey of methods of fabricating 3D periodic dielectric structures can be found in Refs. 87 and 88. As regards magnetic structure fabrication, the so far best developed methods are those of fabricating 1D systems (magnetic multilayers). Below we describe the currently available techniques of 2D and 3D magnonic crystal fabrication. A very promising method is ion implantation applied to ferromagnetic thin films.[89,90] Widely used in submicron semiconductor technology,[91] ion implantation has been applied for *spatial* modulation of anisotropy,[92,93] damping coefficient,[94] and effective gyromagnetic ratio.[89] Ion implantation (with lithographic mask or directed ion beam) allows fabrication of magnonic crystals with either 2D or 3D periodicity.[94] Modeling magnetic properties by light or ion irradiation is discussed in detail in a survey by Fassbender *et al.*[95] There is also an interesting possibility of "optical" fabrication of 3D MCs, based on the effect of local crystallization of Co_2MnSi (due to ferromagnetic phase formation) induced by femtosecond laser pulse. In general, interference of two laser beams can also result in a periodic magnetic structure reproducing the interference pattern.[96]

Two-dimensional periodic structures are also fabricated by lithographic methods, such as e-beam lithography[97] or ultraviolet lithography.[30] A promising technique using porous alumina templates allows fabrication of large regular lattice-based systems of ferromagnetic rods of length 0.2–200 μm with lattice constant ranging from 50 to 500 nm.[98,99] Block copolymer lithography is used as well, allowing fabrication of systems composed of a few nanolayers of periodically distributed magnetic particles with period ~56 nm.[100] The lithographic methods have an advantage of giving an almost free choice of the crystallographic structure of the fabricated 2D MC, with a variety of dot shapes and a wide range of available filling fraction and lattice constant values.[101,102] An excellent survey of methods of fabricating 2D ordered magnetic structures can be found in a paper by Terris and Thomson.[103] Methods of fabricating 2D ordered magnetic nanostructures, with many references, are also discussed in a survey by Martiń *et al.*[104] Worthy of notice are also the self-assembled methods, allowing fabrication of 2D and 3D lattices of Co or Fe nanoparticles.[105–108]

Finally, an important incentive to study magnonic crystals now is their prospective application to the construction of logic systems using the wave nature of spin excitations. Many papers on this subject have been published in recent years, the discussed effects of possible practical application including wave front reversal (phase conjugation) of surface magnetostatic waves,[109] spin-wave interference,[110–112] or the possibilities of controlling spin-wave phase (an analog of the Aharonov-Bohm effect).[113] Other prospective applications are based on negative magnetic refraction coefficient (left-handed spin waves)[114] or magnetostatic wave focusing.[115,116]

The present paper is laid out as follows: Section II presents the general theory of spin-wave propagation in 3D magnonic crystals composed of two different ferromagnetic materials. The scattering centers, either spherical or spheroid shaped, form a cubic crystal lattice, the considered lattice types including sc, bcc, and fcc structures. In each case we report the results of our numerical calculations performed by the plane-wave method and providing a basis for analyzing the effect of material and structural parameter values on the spin-wave spectrum, in particular, on the width of the energy gaps. Section III is focused on the determination of spin-wave dispersion. In Sec. IV we discuss the effect of the structural parameters on the gap width. Its dependence on the magnetic contrast is analyzed in Sec. V. The effect of the scattering center shape on the magnonic band structure is discussed in Sec. VI, in which we consider scattering center deformation eliminating the spherical symmetry of the ferromagnetic clusters. The results of the present study are summarized in Sec. VII.

II. METHOD OF DETERMINING MAGNONIC CRYSTALS SPIN-WAVE SPECTRUM

Band structures of all periodic composites (photonic, phononic, or magnonic crystals) are calculated by similar methods. A commonly used numerical technique is the plane-wave method (PWM), popular because of its conceptual simplicity and applicability to any lattice type and scattering center shape. There are some constraints, however, encountered among others in the case of magnetophotonic crystals, the treatment of which, therefore, requires the use of auxiliary techniques, e.g., perturbation methods, in which the interaction of the electromagnetic field with the ferromagnetic material is regarded as a perturbation.[117]

As the theory of MCs is only in its initial phase of development, the literature on the determination of spin-wave dispersion is as yet limited to the cases of superlattices and magnetic multilayers. The reported calculations are mainly based on the PWM, but other methods have been used as well, including the transfer matrix method,[118,119] the Green function method,[120–122] a technique using effective magnetic parameters,[123] or a microscopic approach based on the Heisenberg Hamiltonian.[44,124] The calculation methods used in the case of 2D and 3D MCs include PWM, averaging methods,[125] the dynamical matrix method,[126] and an approximate method assuming separability of the effective potential.[82] Mills and co-workers published a series of papers on the determination of spin-wave frequencies in 2D lattice-based systems of ferromagnetic cylinders or spheres with dipolar-exchange interactions taken into account on the basis of the solutions obtained for an isolated cylinder or sphere.[127–129]

In the classical approach the spin-wave dispersion relation is determined from the equation of motion of the space- and

time-dependent magnetization vector $\vec{M}(\vec{r},t)$. Referred to as Landau-Lifshitz (LL) equation, it reads

$$\frac{\partial \vec{M}(\vec{r},t)}{\partial t} = \gamma\mu_0 \vec{M}(\vec{r},t) \times \vec{H}_{\text{eff}}(\vec{r},t) + \frac{\alpha}{M_S}\left[\vec{M} \times \frac{\partial \vec{M}(\vec{r},t)}{\partial t}\right], \tag{1}$$

where γ is the gyromagnetic ratio, $\vec{H}_{\text{eff}}$ denotes the effective magnetic field acting on magnetic moments, and the last term on the right describes relaxation with dimensionless damping factor α. The above LL equation is written in SI units, with μ_0 denoting the permeability of vacuum [in the case of free electrons we can assume $\gamma\mu_0 \approx 2.21 \times 10^5$ $(\text{A/m})^{-1}$ s^{-1}]. Although some of the damping effects in 1D MCs have already been discussed in the literature,[130,131] the relaxation processes are neglected in the calculations performed in this study.

The effective magnetic field $\vec{H}_{\text{eff}}$ acting on magnetic moments in an MC is in general a sum of several components, which can all be space dependent,

$$\vec{H}_{\text{eff}}(\vec{r},t) = \vec{H}_0 + \vec{H}_{\text{ani}} + \vec{H}_{\text{ex}} + \vec{H}_{\text{ms}}. \tag{2}$$

The first component of $\vec{H}_{\text{eff}}$ is the applied magnetic field $\vec{H}_0$; let us assume it to be *homogeneous* in space, and strong enough to enforce parallel alignment of all the magnetic moments. Should this applied magnetic field be periodic in space, its periodicity would result in a periodic potential with barriers and wells for spin waves; such structure, considered by Bayer *et al.*,[121] could be itself regarded as magnonic. However, in this study we focus on structures of magnonic nature only due to material nonhomogeneity.

Another component of the effective field is the anisotropy field $\vec{H}_{\text{ani}}$, which can vary between the constituent materials. One-dimensional magnonic structures owing their magnonic nature to a periodicity of the anisotropy field have been investigated by Kuchko and co-workers.[45,84] However, the difference in $\vec{H}_{\text{ani}}$ values between the constituent materials tends to be slight, and thus the effect of this nonhomogeneity is usually minor; therefore, we shall henceforth assume this component to be negligible.

The next component of the effective field is the exchange field $\vec{H}_{\text{ex}}$. In magnetically nonhomogeneous materials both the spatial nonhomogeneity of the exchange stiffness constant $A(\vec{r})$, and that of the spontaneous magnetization $M_S(\vec{r})$ must be taken into account, which leads to the following formula:

$$\vec{H}_{\text{ex}}(\vec{r},t) = (\nabla \cdot \lambda_{\text{ex}}^2(\vec{r},t)\,\nabla)\vec{M}(\vec{r},t) \quad \text{where } \lambda_{\text{ex}} = \sqrt{\frac{2A}{\mu_0 M_S^2}}; \tag{3}$$

λ_{ex} is the exchange length, A is the exchange stiffness constant, and M_S denotes the spontaneous (saturation) magnetization.

The last component of the effective magnetic field is the magnetostatic interaction field $\vec{H}_{\text{ms}}$. In the case considered in this study, i.e., in an infinite 3D lattice of ferromagnetic spheroids embedded in a ferromagnetic matrix, the nonuniform static demagnetization field can be assumed to be (see, e.g., Refs. 132 and 133) homogeneously averaged throughout the magnonic crystal, which implies that the only components of the magnetostatic field to be treated in the calculations as *spatially dependent* are the dynamic ones (perpendicular to the direction of the applied field). This approximation is justified since we are mainly interested in the energy gaps in the magnetic excitation spectra of magnonic crystals. In the magnetostatic approximation (with relaxation effects neglected) this dynamic magnetic field must fulfill the magnetostatic Maxwell's equations as follows:

$$\nabla \times \vec{h}(\vec{r},t) = 0,$$

$$\nabla \cdot (\vec{h}(\vec{r},t) + \vec{m}(\vec{r},t)) = 0, \tag{4}$$

where $\vec{m}(\vec{r},t)$ is the magnetization vector component perpendicular to $\vec{H}_0$: $\vec{M}(\vec{r},t) = M_z(\vec{r})\hat{z} + \vec{m}(\vec{r},t)$. Thus the formula for the effective field takes the following form we shall henceforth use in this paper:

$$\vec{H}_{\text{eff}}(\vec{r},t) = H_0\hat{z} + \vec{h}(\vec{r},t) + (\nabla \cdot \lambda_{\text{ex}}^2\,\nabla)\vec{M}(\vec{r},t). \tag{5}$$

Let us solve the LL vector equation (1) with effective field (5) in the linear approximation, i.e., assuming all terms with squared $\vec{m}(\vec{r},t)$ and $\vec{h}(\vec{r},t)$ to be negligible. This approximation is equivalent to assuming the magnetization vector component parallel to the constant magnetic field is constant in time and of value much greater than those of the perpendicular components: $|\vec{m}(\vec{r},t)| \ll M_z(\vec{r})$; thus, we can assume $M_z \approx M_S$. In search of solutions corresponding to monochromatic spin waves, $\vec{m}(\vec{r},t) \sim \exp(i\omega t)$ (ω being the wave frequency), using the linear approximation, we derive the following system of equations from Eqs. (1) and (4):

$$i\Omega m_x(\vec{r}) + \frac{1}{H_0} M_S[\vec{\nabla} \cdot \lambda_{\text{ex}}^2 \vec{\nabla}] m_y(\vec{r}) - m_y(\vec{r}) - \frac{1}{H_0} m_y(\vec{r}) \times [\vec{\nabla} \cdot \lambda_{\text{ex}}^2 \vec{\nabla}] M_S + \frac{M_S}{H_0}\frac{\partial \psi(\vec{r})}{\partial y} = 0, \tag{6}$$

$$i\Omega m_y(\vec{r}) - \frac{1}{H_0} M_S[\vec{\nabla} \cdot \lambda_{\text{ex}}^2 \vec{\nabla}] m_x(\vec{r}) + m_x(\vec{r}) + \frac{1}{H_0} m_x(\vec{r}) \times [\vec{\nabla} \cdot \lambda_{\text{ex}}^2 \vec{\nabla}] M_S - \frac{M_S}{H_0}\frac{\partial \psi(\vec{r})}{\partial x} = 0, \tag{7}$$

$$\nabla^2 \psi(\vec{r}) - \left[\frac{\partial m_x(\vec{r})}{\partial x} + \frac{\partial m_y(\vec{r})}{\partial y}\right] = 0, \tag{8}$$

where Ω denotes the dimensionless *reduced frequency* defined as

$$\Omega = \frac{\omega}{|\gamma|\mu_0 H_0}. \tag{9}$$

Equation (8) is derived from Maxwell's equations (4) by introducing the magnetostatic potential $\psi(\vec{r},t)$ fulfilling equation $\vec{h}(\vec{r},t) = -\nabla\psi(\vec{r},t)$.

Crucial for the magnonic nature of the considered structure is the assumption that the material parameters in the above equations, namely, A and M_S, and consequently also λ_{ex}^2, are periodic functions of the position vector $\vec{r}=(x,y,z)$, with period equal to the lattice vector $\vec{a}$ as follows:

$$M_S(\vec{r}+\vec{a}) = M_S(\vec{r}), \quad A(\vec{r}+\vec{a}) = A(\vec{r}), \quad \text{and} \quad \lambda_{ex}^2(\vec{r}+\vec{a}) = \lambda_{ex}^2(\vec{r}). \tag{10}$$

In MCs composed of two materials each of these material parameters can be expressed by two terms representing its respective values in each constituent material as follows:

$$M_S(\vec{r}) = M_{S,B} + (M_{S,A} - M_{S,B})S(\vec{r}),$$

$$\lambda_{ex}^2(\vec{r}) = \lambda_{ex,B}^2 + (\lambda_{ex,A}^2 - \lambda_{ex,B}^2)S(\vec{r}); \tag{11}$$

subscripts A or B refer to the scattering centers and the matrix, respectively; $S(\vec{r})$ is a function that takes on value 1 for vector $\vec{r}$ indicating any point in material A, and value 0 beyond.

Let us use the plane-wave method to solve the system of Eqs. (6)–(8). The method is based on Bloch's theorem, which asserts that a solution of a differential equation with periodic coefficients can be represented as a product of a plane-wave envelope function and a periodic Bloch function as follows:

$$\vec{m}(\vec{r}) = \vec{m}_{\vec{k}}(\vec{r})e^{i\vec{k}\cdot\vec{r}} = \sum_{\vec{G}} \vec{m}_{\vec{k}}(\vec{G})e^{i(\vec{k}+\vec{G})\cdot\vec{r}},$$

$$\psi(\vec{r}) = \psi_{\vec{k}}e^{i\vec{k}\cdot\vec{r}} = \sum_{\vec{G}} \psi_{\vec{k}}(\vec{G})e^{i(\vec{k}+\vec{G})\cdot\vec{r}}, \tag{12}$$

where

$$\vec{m}_{\vec{k}}(\vec{r}+\vec{a}) = \vec{m}_{\vec{k}}(\vec{r}) \quad \text{and} \quad \psi_{\vec{k}}(\vec{r}+\vec{a}) = \psi_{\vec{k}}(\vec{r}); \tag{13}$$

$\vec{k}$ is a wave vector in the first Brillouin zone and $\vec{G}$ denotes a reciprocal lattice vector. The next step is the Fourier transform that maps the periodic functions M_S and λ_{ex}^2 in Eqs. (6)–(8) to the reciprocal space. The transformation formulas are as follows:

$$M_S(\vec{r}) = \sum_{\vec{G}} M_S(\vec{G})e^{i\vec{G}\cdot\vec{r}}, \quad \lambda_{ex}^2(\vec{r}) = \sum_{\vec{G}} \lambda_{ex}^2(\vec{G})e^{i\vec{G}\cdot\vec{r}}. \tag{14}$$

Including expansions (12)–(14) into Eq. (8) allows us to express the Fourier components of the magnetostatic potential by the components of the dynamic magnetization as follows:

$$\psi_{\vec{k}}(\vec{G}) = -i\frac{(k_x+G_x)m_{x\vec{k}}(\vec{G}) + (k_y+G_y)m_{y\vec{k}}(\vec{G})}{(\vec{k}+\vec{G})^2}, \tag{15}$$

where k_x, k_y and G_x, G_y denote the x and y components of wave vector $\vec{k}$ and reciprocal lattice vector $\vec{G}$, respectively, in the Cartesian system of coordinates; $m_{x,\vec{k}}(\vec{G})$ and $m_{y,\vec{k}}(\vec{G})$ are Fourier coefficients in the expansion (12) of the dynamic magnetization components.

By including transforms (12)–(14) and formula (15) into Eqs. (6) and (7), the following infinite system of equations is obtained:

$$i\Omega m_{x\vec{k}}(\vec{G}) = m_{y\vec{k}}(\vec{G}) + \sum_{\vec{G}'} \frac{(k_y+G_y')(k_x+G_x')m_{x\vec{k}}(\vec{G}') + (k_y+G_y')^2 m_{y\vec{k}}(\vec{G}')}{H_0|\vec{k}+\vec{G}'|^2} M_S(\vec{G}-\vec{G}') + \frac{1}{H_0}\sum_{\vec{G}'}\sum_{\vec{G}''}[(\vec{k}+\vec{G}')\cdot(\vec{k}+\vec{G}'') - (\vec{G}-\vec{G}'')\cdot(\vec{G}-\vec{G}')]M_S(\vec{G}-\vec{G}'')\lambda_{ex}^2(\vec{G}''-\vec{G}')m_{y\vec{k}}(\vec{G}'),$$

$$i\Omega m_{y\vec{k}}(\vec{G}) = -m_{x\vec{k}}(\vec{G}) - \sum_{\vec{G}'} \frac{(k_y+G_y')(k_x+G_x')m_{y\vec{k}}(\vec{G}') + (k_x+G_x')^2 m_{x\vec{k}}(\vec{G}')}{H_0|\vec{k}+\vec{G}'|^2} M_S(\vec{G}-\vec{G}') - \frac{1}{H_0}\sum_{\vec{G}'}\sum_{\vec{G}''}[(\vec{k}+\vec{G}')\cdot(\vec{k}+\vec{G}'') - (\vec{G}-\vec{G}'')\cdot(\vec{G}-\vec{G}')]M_S(\vec{G}-\vec{G}'')\lambda_{ex}^2(\vec{G}''-\vec{G}')m_{x\vec{k}}(\vec{G}'). \tag{16}$$

Found from the transform inverse to Eq. (14), the Fourier coefficients of the material parameters $M_S(\vec{G})$ and $\lambda_{ex}^2(\vec{G})$ in these equations read

$$M_S(\vec{G}) = \frac{1}{V_c}\int_{V_c} M_S(\vec{r})e^{-i\vec{G}\cdot\vec{r}}d^3r, \tag{17}$$

$$\lambda_{ex}^2(\vec{G}) = \frac{1}{V_c}\int_{V_c} \lambda_{ex}^2(\vec{r})e^{-i\vec{G}\cdot\vec{r}}d^3r. \tag{18}$$

These coefficients can be calculated either by integration over the unit cell volume V_c or determined numerically by means of the fast Fourier transform in a procedure similar to that used for the determination of photonic band structures.[134] In the case of spheroids of semiaxes σ_x, σ_y, and σ_z analytical integration can be performed,[135] yielding the following formulas:

$$M_S(\vec{G}) = \begin{cases} M_{S,A}f + M_{S,B}(1-f) & \text{for } \vec{G}=0 \\ f(M_{S,A}-M_{S,B})\dfrac{3[\sin(P)-(P)\cos(P)]}{(P)^3} & \text{for } \vec{G}\neq 0, \end{cases} \tag{19}$$

where $P=\sqrt{(\sigma_x G_x)^2+(\sigma_y G_y)^2+(\sigma_z G_z)^2}$, and f is the filling fraction, i.e., the volume proportion of material A in a unit cell. Obviously, $\sigma_x=\sigma_y=\sigma_z=R$ in the case of spheres of radius R.

When a finite number N of reciprocal lattice vectors is used in the Fourier series (14), also the system of Eq. (16) becomes finite. Its structure corresponds to an eigenproblem with eigenvalues $i\Omega$ and eigenvectors $m_{x,\vec{k}}(\vec{G})$ and $m_{y,\vec{k}}(\vec{G})$. The eigenproblem at hand can also be put in the matrix form (indexed with reciprocal lattice vectors $\vec{G}_i$) as follows:

$$\hat{M}\vec{m}_{\vec{k}} = i\Omega\vec{m}_{\vec{k}}, \tag{20}$$

with the eigenvector defined $\vec{m}_{\vec{k}}^T = [m_{x,\vec{k}}(\vec{G}_1),\ldots,m_{x,\vec{k}}(\vec{G}_N),m_{y,\vec{k}}(\vec{G}_1),\ldots,m_{y,\vec{k}}(\vec{G}_N)]$; the matrix of this eigenproblem is the following block matrix:

$$\hat{M} = \begin{pmatrix} \hat{M}^{xx} & \hat{M}^{xy} \\ \hat{M}^{yx} & \hat{M}^{yy} \end{pmatrix}. \tag{21}$$

The submatrices in Eq. (21) are defined as follows:

$$\hat{M}_{ij}^{xx} = -\hat{M}_{ij}^{yy} = \frac{(k_y+G_{y,j})(k_x+G_{x,j})}{H_0|\vec{k}+\vec{G}_j|^2} M_S(\vec{G}_i-\vec{G}_j), \tag{22}$$

$$\hat{M}_{ij}^{xy} = \delta_{ij} + \sum_l \frac{[(\vec{k}+\vec{G}_j)\cdot(\vec{k}+\vec{G}_l)-(\vec{G}_i-\vec{G}_l)\cdot(\vec{G}_i-\vec{G}_j)]}{H_0} \times \lambda_{\text{ex}}^2(\vec{G}_l-\vec{G}_j)M_S(\vec{G}_i-\vec{G}_l) + \frac{(k_y+G_{y,j})^2}{H_0|\vec{k}+\vec{G}_j|^2} \times M_S(\vec{G}_i-\vec{G}_j), \tag{23}$$

$$\hat{M}_{ij}^{yx} = -\delta_{ij} - \sum_l \frac{[(\vec{k}+\vec{G}_j)\cdot(\vec{k}+\vec{G}_l)-(\vec{G}_i-\vec{G}_l)\cdot(\vec{G}_i-\vec{G}_j)]}{H_0} \times \lambda_{\text{ex}}^2(\vec{G}_l-\vec{G}_j)M_S(\vec{G}_i-\vec{G}_l) - \frac{(k_x+G_{x,j})^2}{H_0|\vec{k}+\vec{G}_j|^2} \times M_S(\vec{G}_i-\vec{G}_j), \tag{24}$$

where reciprocal lattice vector indices i, j, and l are integers in the range $\langle 1,N\rangle$.

We shall solve the system of Eq. (20) by standard numerical procedures designed for solving real matrix eigenproblems. It should be kept in mind, however, that all eigenvalues found by these procedures must be put to the convergence test. For all structures considered, satisfactory convergence of numerical solutions of Eq. (20) proves to be attained with the use of 1331 reciprocal lattice vectors.[136]

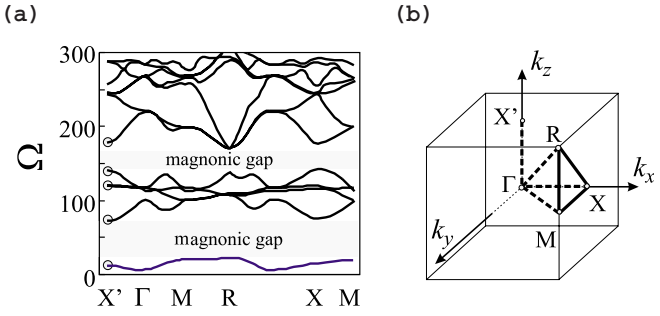

FIG. 1. (Color online) (a) The magnonic band structure of sc MC with lattice constant $a=100$ Å. The MBS is plotted along the path in the first Brillouin zone represented by the bold line in (b). The MC is composed of Fe spheres of radius $R=26.28$ Å disposed in sites of the sc lattice and embedded in YIG. Gray circles indicate the beginnings of the first five branches [at point corresponding to wave vector $\vec{k}=2\pi/a(0,0,0.5)$]. The assumed magnetic field value is $\mu_0 H_0=0.1$ T.

III. sc MAGNONIC CRYSTALS

In this section we shall consider magnonic band structures (MBSs) obtained in MCs with spherical-shaped ferromagnetic scattering centers forming an sc lattice. An example of MBS resulting from the numerical solution of the eigenproblem (20) for such an MC is shown in Fig. 1(a). The assumed value of the sc lattice constant is $a=100$ Å; the magnetic parameters of the matrix material are close to those of YIG: $M_{S,A}=0.194\times 10^6$ A m^{-1} and $\lambda_{\text{ex}}=130$ Å; the magnetic parameters of the ferromagnetic material of the spherical scattering centers correspond to iron: $M_{S,A}=1.752\times 10^6$ A m^{-1} and $\lambda_{\text{ex}}=33$ Å. The filling fraction value assumed in the calculations, $f=0.2$, corresponds to sphere radius $R=26.28$ Å. The MBS shown in Fig. 1(a) is plotted along the path in the first Brillouin zone represented by the bold line in Fig. 1(b). The two magnonic gaps in the resulting spectrum represent the frequency ranges in which spin waves are forbidden from propagating. The lower MG occurs between the first branch and the second one, while the upper gap is found between the fifth and the sixth ones. Below we investigate the mechanism of gap opening by analyzing the amplitude profiles of spin waves corresponding to these branches.

The solution of Eq. (20) yields both eigenfrequencies and eigenvectors $\vec{m}_{\vec{k}}$, the latter being the Fourier coefficients of the dynamic magnetization components. Spatial profiles of these components can be determined on the basis of Bloch's theorem (12) and the eigenvectors found as follows:

$$m_{x(y)}(\vec{r}) = \sum_{\vec{G}} m_{x(y)\vec{k}}(\vec{G})e^{-i(\vec{k}+\vec{G})\cdot\vec{r}}. \tag{25}$$

Figures 2 and 3 show profiles of squared dynamic magnetization component, $|m_x(\vec{r})|^2$, for $\vec{r}$ indicating points within a selected area in planes (001) and (002) (depicted in Fig. 2) and at wave vector $\vec{k}=2\pi/a(0,0,0.5)$, corresponding to point X' in the Brillouin zone.

The first branch in the magnonic spectrum is seen to correspond to a spin-wave excitation in the Fe spheres with maximum amplitude m_x at the sphere center [plane (001) in

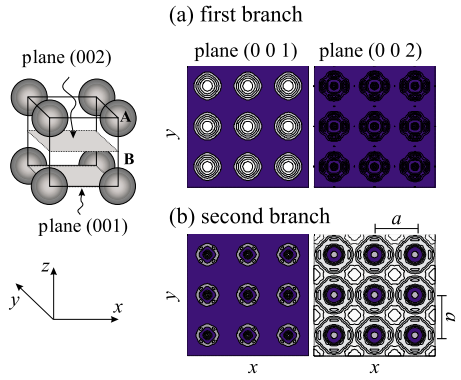

FIG. 2. (Color online) Profiles of squared dynamic magnetization component, $|m_x(\vec{r})|^2$, in two adjacent planes, (002) and (001) (right and left column, respectively); the planes are shown on the left. White color corresponds to maximum values of amplitudes $|m_x(\vec{r})|^2$. The amplitudes in branches I and II are shown in (a) and (b), respectively; in both cases $\vec{k}=2\pi/a(0,0,0.5)$. The MC is composed of Fe spheres disposed in sites of an sc lattice and embedded in YIG; the assumed parameter values are lattice constant $a=100$ Å and sphere radius $R=26.28$ Å. The depicted areas are indicated by the position vector of x and y components: $x \in \langle -1.5a, 1.5a \rangle$ and $y \in \langle -1.5a, 1.5a \rangle$.

Fig. 2(a)]. Note the other plane, (002), crossing the z axis at value 0.5, cuts across the matrix material only; therefore, the second branch corresponds to a spin-wave excitation propagating mainly in the matrix. Both spin waves have maximum amplitude at point (0,0,0) in Fe (branch I) and at point (0.5,0.5,0.5) in YIG (branch II). The first magnonic gap is thus delimited by the two lowest spin-wave excitations, one localized in the Fe spheres and the other in the matrix (branches I and II, respectively).

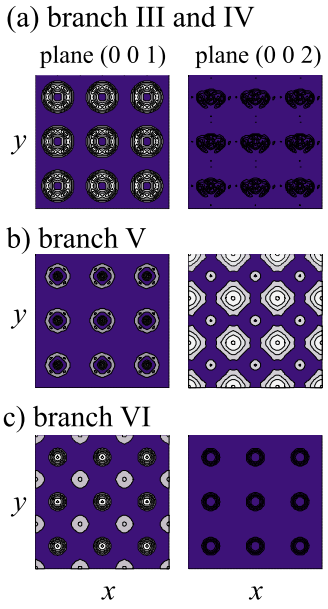

FIG. 3. (Color online) Spatial profiles of squared dynamic magnetization component, $|m_x(\vec{r})|^2$, in planes (002) and (001) (right and left column, respectively), branches III and IV (a), V (b), and VI (c). All the structural and magnetic parameter values are as in Fig. 2.

Profiles of squared magnetization $|m_x(\vec{r})|^2$ in higher branches, at the same Brillouin zone boundary wave vector, $\vec{k}=2\pi/a(0,0,0.5)$, are depicted in Fig. 3 the squared amplitudes in each branch are normalized to their branch maximum). Branches III and IV are degenerated at X' and along the path $X' \rightarrow \Gamma$ (see Fig. 1), and the amplitude of the corresponding spin waves is nonzero only in the Fe spheres. These spin waves are the lowest antisymmetric excitations with amplitude vanishing in the sphere centers and reaching minimum in directions (100) and (010). It is only between the next two branches, V and VI, that the upper magnonic gap is found to open. The squared amplitudes of the dynamic magnetization components in each of these branches are shown in Figs. 3(b) and 3(c). In both bands the amplitude is nonzero in the sphere center (0,0,0) as well as in the "matrix center" (0.5, 0.5, 0.5), with YIG excitations prevailing in branch V, and Fe excitations predominant in branch VI. Thus, the mechanism of the second magnonic gap opening is similar to that of the first gap opening, and we can expect both to be determined by a material parameter contrast between the constituent materials, analogously to the case of photonic crystals[134] (in the case of magnonic crystals the contrasts in question are those of magnetization and exchange length values).

Before closing this section, let us look into the nature of the lowest branch. When the corresponding excitation is localized mainly in the ferromagnetic spheres, the spin-wave vector can be assumed to be $k_{SW}=2\pi/\lambda=2\pi R/4$ (the mode in question is assumed to represent the fundamental mode); for $R=26.28$ Å we get $k_{SW} \approx 5 \times 10^6$ cm^{-1}. At wave vector values as high as that the exchange energy component (proportional to k^2) is predominant, and consequently, the excitation can be qualified as exchange dominated.

IV. MAGNONIC SPECTRUM VERSUS CRYSTALLOGRAPHIC STRUCTURE

In this section we compare the width of respective MGs in the magnonic spectra of three cubic structures (sc, fcc, and bcc) and examine the dependence of the gap width on the structural parameters of the composite material (the dependence on the material parameters is discussed in the next section).

Let us first scrutinize the effect of the *filling fraction*, f, defined as the volume proportion of the ferromagnetic spheres in a unit cell. For each of the three lattice types considered, we get the respective formulas relating the filling fraction and the sphere radius R:

$$f_{sc} = \frac{4\pi R^3}{3a^3}, \quad f_{bcc} = \frac{8\pi R^3}{3a^3}, \quad f_{fcc} = \frac{16\pi R^3}{3a^3}. \tag{26}$$

Note f takes on values within the range $(0, f_{max})$, value $f=0.0$ corresponding to a homogeneous ferromagnet (the matrix material), and f_{max} to a densely packed structure with spheres touching one another. It is easy to show that f_{max} takes on the following different values in each of the three structure types:

$$f_{sc,max} \approx 0.52, \quad f_{bcc,max} \approx 0.68, \quad f_{fcc,max} \approx 0.74. \tag{27}$$

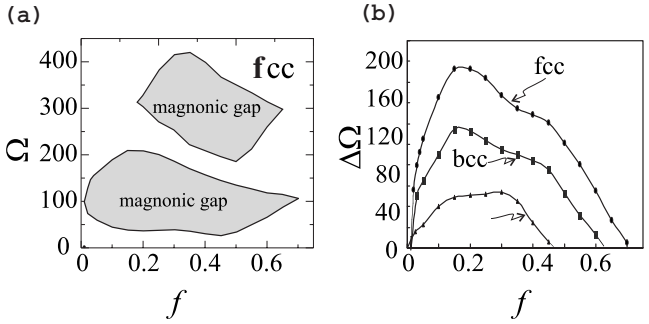

FIG. 4. (a) The structural evolution of MGs in fcc MC with spherical-shaped Fe scattering centers embedded in a YIG matrix; f denotes the filling fraction. (b) Superimposed plot of the lower gap width versus the filling fraction in sc, bcc, and fcc structures; in all the three lattice types considered the assumed lattice constant value is $a=100$ Å.

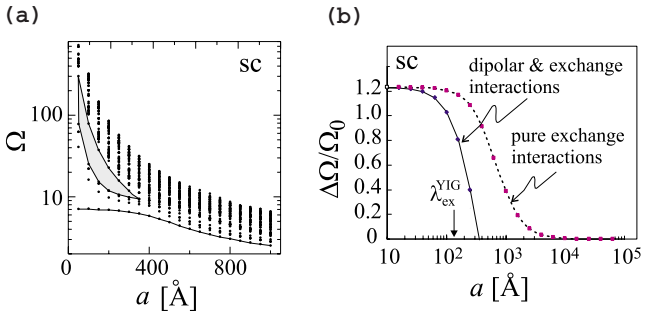

FIG. 5. (Color online) (a) The magnonic spectrum evolution with increasing lattice constant a in sc MC (Fe spheres embedded in YIG, filling fraction $f=0.2$); the shaded region represents the MG between branches I and II. (b) The MG width (normalized to the gap center Ω_0) plotted versus a; the solid line represents results obtained from the solution of the complete eigenproblem (20), i.e., with both dipolar and exchange interaction energies taken into account; the dotted line is plotted with the assumption of negligible magnetostatic interaction energy [$\hat{M}^{xx}=\hat{M}^{yy}=0$ and the last terms in Eqs. (23) and (24) dropped].

Figure 4(a) shows the magnonic gaps versus the filling fraction in the fcc structure; an analogous plot for the sc structure can be found in our earlier paper.[137] Only two MGs are depicted here: the one between the first and the second branch, and the other between the fourth and the fifth branch. As the latter MG lies at very high frequency region, we will not investigate it in this paper (a recently proposed experiment[138] allows investigation of spin waves of length in the order of nanometers propagating in MCs). The lower energy gap is seen to subsist almost in the whole range of filling fraction values, and its center to remain on nearly constant level. In Fig. 4(b) the width of this first gap is plotted versus f for the three lattice types (sc, bcc, and fcc), at $a=100$ Å and $\mu_0 H_0=0.1$ T. The gap is the widest in the most densely packed structure (fcc), and the narrowest in the sc structure; its maximum value is reached at $f\approx 0.17$ in the fcc structure; the maximum values in the other two lattice types occur at $f\approx 0.15$ and $f\approx 0.3$ in bcc and sc structures, respectively.

Let us now fix the filling fraction at value $f=0.2$ to examine the dependence of the gap width on the lattice constant a. Figure 5(a) shows frequency spectra obtained for a series of a values (the reduced frequency values are presented on a logarithmic scale). The shaded area represents the first MG, and the solid line the bottom of the first magnonic band (corresponding to point Γ). As expected, the spin-wave frequency spectrum slopes down as the lattice constant increases, and the gap vanishes around $a=350$ Å as a result of branch intersection.

The existence of a critical lattice constant value a_{crit} above which the gap does not exist has its specific physical meaning, which we shall formulate with the help of Fig. 5(b). Shown in this figure, the plot of the gap width versus the lattice constant in the situation depicted in Fig. 5(a), in which both dipolar and exchange interactions are taken into account, is superimposed on the plot of the same dependence, but obtained with dipolar interactions neglected. In the case of pure exchange interactions the energy gap is seen to vanish practically at $a\to\infty$, which is easily explicable by the insignificance of the magnetic contrasts in a structure in which the scattering centers are so widely spaced. The comparison of the two curves indicates the dipolar interactions, when taken into account, reduce the "gap-generating" effect of the magnetic contrasts, which is due to exchange interactions. This destructive effect of the dipolar interactions increases with a and results in closing the gap at $a>a_{\text{crit}}$. On the other hand, note that the effect of the dipolar interactions on the gap width is of little importance as long as the lattice constant remains below the matrix exchange length ($\lambda_{\text{ex}}^{\text{YIG}}\approx 130$ Å), while at lattice constant value close to twice the value of the exchange length the gap vanishes.

V. EFFECT OF MAGNETIC CONTRASTS ON THE MAGNONIC GAP WIDTH

Let us examine the effect of magnetic parameters of the constituent materials on MBS and MG by considering hypothetical systems with magnetic parameters M_S, A, and λ_{ex}, of the constituent materials taking on values within a realistic range, yet not correlated with any real material.

The first dependence to be investigated is that of the MG width on the exchange contrast stemming from a difference between the values of the exchange stiffness constant in the ferromagnetic spheres and in the matrix material; the two values are denoted A_A and A_B, respectively. The calculation scheme is based on the assumption of constant values of the magnetic parameters in the matrix ($M_{S,B}=0.194\times 10^6$ A m^{-1}, $A_B=0.4\times 10^{-11}$ J m^{-1}) and constant value of spontaneous magnetization in the spheres ($M_{S,A}=1.752\times 10^6$ A m^{-1}), the only variable parameter being the exchange stiffness A_A in the spheres; all the relations under investigation will be plotted versus the exchange stiffness ratio, A_A/A_B. Also the structural parameters are assumed constant in this section, their values remaining as fixed above (lattice constant $a=100$ Å, filling fraction $f=0.2$, and applied magnetic field $\mu_0 H_0=0.1$ T).

In the plot shown in Fig. 6(a) the width of the first magnonic gap in the fcc structure is seen to increase with the

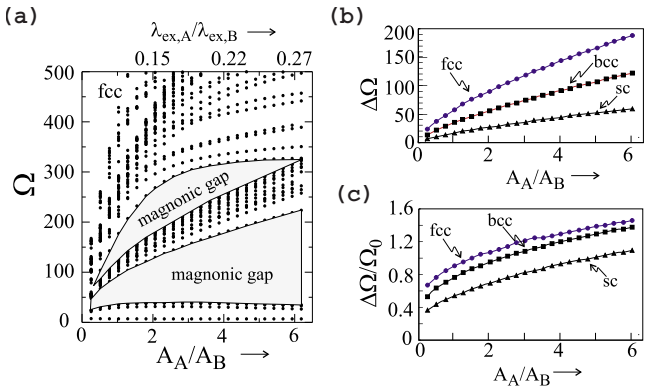

FIG. 6. (Color online) (a) The magnonic spectrum in fcc structure versus the exchange contrast defined as either the ratio A_A/A_B of the exchange stiffness constant values in the constituent materials (bottom scale) or the ratio of the respective exchange length values (top scale). Shaded regions represent MGs. (b) The width and (c) the normalized width of the lower MG as a function of the exchange contrast for sc, bcc, and fcc lattices (triangles, squares, and circles, respectively). Mind the exchange contrast is only controlled by changing the value of the exchange stiffness A_A in the spheres, all the other parameters being fixed: $A_B=0.4\times10^{-11}$ J m^{-1}, $M_{S,A}=1.752\times10^6$ A m^{-1}, $M_{S,B}=0.194\times10^6$ A m^{-1}, $a=100$ Å, $f=0.2$, and $\mu_0H_0=0.1$ T.

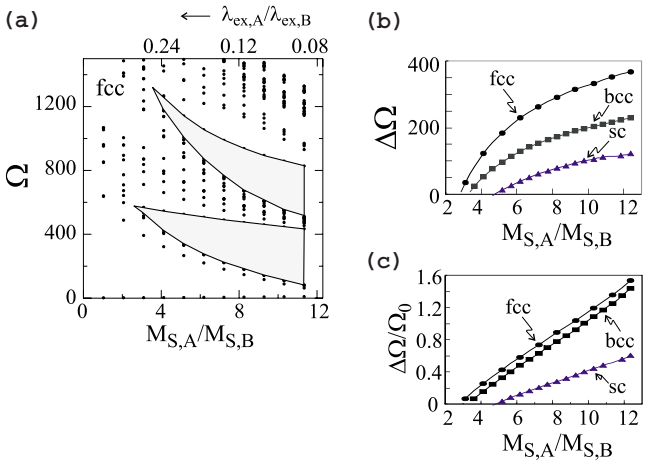

FIG. 7. (Color online) (a) The magnonic spectrum versus the magnetization contrast defined as the ratio $M_{S,A}/M_{S,B}$ of the spontaneous magnetization values in the constituent materials. Shaded regions represent MGs. (b) The width of the lower MG versus the magnetization contrast for sc, bcc, and fcc lattices (triangles, squares, and circles, respectively). Mind the magnetization contrast is only controlled by changing the value of magnetization $M_{S,A}$ in the spheres, all the other parameters being fixed: $A_A=A_B=2.1\times10^{-11}$ J m^{-1}, $M_{S,B}=0.194\times10^6$ A m^{-1}, $a=100$ Å, $f=0.2$, and $\mu_0H_0=0.1$ T.

exchange contrast $\lambda_{ex,A}/\lambda_{ex,B}$. This rule applies to the other structures as well [see Fig. 6(b)], but it is in the fcc MC that the gap widening is the most dynamic. Note, however, that the dependence of the *normalized* gap width to the exchange contrast is *the same* (and *nearly linear*) in all three structure types, as indicated by Fig. 6(c). Worthy of notice is also the existence of the MG at any value of the exchange contrast (both above and below 1) at the assumed magnetic contrast value (different from 1).

The effect of the spontaneous magnetization contrast is depicted in Fig. 7. The values of the exchange stiffness constant in both constituent materials are assumed to be equal ($A_A=A_B=2.1\times10^{-11}$ J m^{-1}); the magnetization contrast is controlled by regulating the magnetization value in the spheres, the magnetization in the matrix being fixed at $M_{S,B}=0.194\times10^6$ A m^{-1}. The dependence of the gap width on the magnetization contrast is found to be qualitatively similar to the above-discussed dependence on the exchange contrast. However, their mechanisms must be different, as suggested by the fact that *increasing* the magnetization contrast is equivalent to *reducing* the exchange length contrast. There is also an important difference consisting in the impossibility of gap opening below a certain critical value of magnetization contrast. In Fig. 7 this critical value is seen to depend on the lattice type; we found its value to be 2.8 in sc, 3.2 in bcc, and 4.8 in fcc. Increasing the magnetization contrast above the critical value results in gap widening, and the gap width is seen to asymptotically approach a limit value which is also dependent on the lattice type.

VI. EFFECT OF SCATTERING CENTER SHAPE ON MAGNONIC GAP

Wide possibilities of modeling magnonic crystal properties are offered by controlling the shape of the scattering centers distributed in sites of a crystallographic lattice. The effect of the shape of ferromagnetic scattering centers on static magnetic properties of periodic 2D structures is discussed in a survey by Cowburn.[139] Two major factors contribute to the impact of the scattering center shape on the magnonic spectrum: (1) in an isolated ferromagnetic material the spin-wave spectrum (the set of discrete spin-wave energy levels) strongly depends on the boundary conditions; in a magnonic crystal comprising a system of interacting scattering centers the discrete levels split to form magnonic bands; (2) the other factor is related to the magnetic poles present on the surface of a ferromagnet and creating a nonhomogeneous magnetic field inside the sample. Both factors result in complicated dispersion relations in the case of periodic system of interacting clusters.

Here we shall examine the effect of the ferromagnetic center shape on the magnonic gap width; however, we shall restrict ourselves to the case of spheroid-shaped magnetic grains. The Fourier coefficients of the periodic functions in the eigenproblem (20) can be determined from the analytical formula (19). Let us set the z axis and the σ_z semiaxis along the direction of the applied magnetic field; the other two semiaxes are assumed to be equal: $\sigma_x=\sigma_y$. As regards the material parameters, let us assume the scattering centers are made of Fe and embedded in an YIG matrix, in which they form a lattice with lattice constant $a=100$ Å.

The effect of spheroid deformation, expressed by the semiaxis ratio σ_z/σ_x, is shown in Fig. 8. Note that the value $\sigma_z/\sigma_x=1$ corresponds to spheres, and thus to the case discussed in the previous sections. It is around this value that the fcc and bcc structures show MGs of maximum width; only in the sc structure, in which the MG is the narrowest, its maximum width occurs at $\sigma_z/\sigma_x=0.7$. Therefore, the conclu-

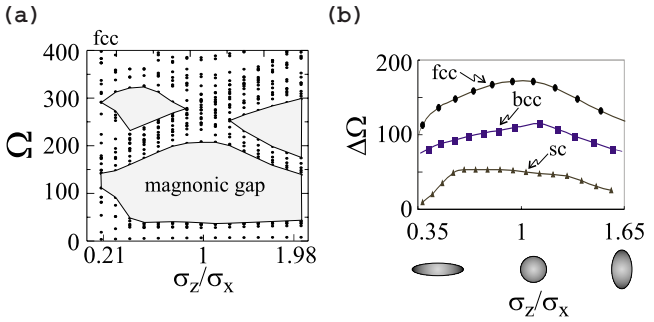

FIG. 8. (Color online) The MBS (a) and the MG width (b) versus spheroid deformation expressed by the semiaxis ratio σ_z/σ_x. The considered structure consists of spheroid-shaped Fe centers embedded in YIG; the assumed filling fraction value is $f=0.2$. (a) Magnonic frequency spectra obtained for fcc MC, plotted versus σ_z/σ_x; shaded regions represent MGs. (b) Superimposed plot of MG width versus σ_z/σ_x in sc, bcc, and fcc MCs.

sion can be drawn that diverging from the spherical symmetry of the ferromagnetic scattering centers leads to a *reduction* of the width of the lower MG (which opens as a result of the presence of the scattering centers). It is an important finding, as it implies that modeling of the scattering center shape could be of much use in attempts to match theoretical results to experimental ones. Such an attempt is reported in our previous paper,[140] in which we postulate, on the basis of such model considerations, the magnonic origin of the gap found to occur in spin-wave spectra of doped manganites.

VII. CONCLUSION

This paper is an introduction to the theory of magnonic crystals, and hopefully a good starting point for research in magnonic structures more complex than those considered in this study. We have investigated two-component magnonic crystals with spheroid-shaped scattering centers forming a cubic (sc, fcc, and bcc) lattice. The constituent materials are ferromagnets of different magnetic properties; different values of the exchange constant and the spontaneous magnetization in each of them create the magnetic contrasts which are the origin of the magnonic nature of the considered structures. Determined numerically by the plane-wave method (adopted from the theory of photonic crystals), the presented magnonic spectra reveal energy gaps, i.e., frequency ranges in which spin waves are forbidden from propagating. Both magnetic contrasts are of key importance for magnonic gap opening; the spontaneous magnetization contrast proves a sufficient condition for magnonic gaps to open, provided its value is above a certain critical level, which depends on the lattice type. As regards the exchange contrast, it has an important effect on the gap width, but needs to take on very large values to cause magnonic gap opening in the absence of magnetization contrast. The almost linear dependence of the normalized magnonic gap on each of the two magnetic contrasts considered could be of some practical use in materials science, as it provides a simple way of modeling the width of the lowest magnonic band by controlling the magnetic contrasts.

We have ascertained that the crystallographic structure plays an important role in the creation of magnonic gaps, as the best conditions of gap opening are offered by the lattices of the highest packing density. Moreover, the results of our calculations indicate that the gap width is substantially affected by the scattering center shape; in fcc and bcc structures the gaps are found to be the widest when the scattering center shape is close to a sphere. Equally important is the lattice constant: in the considered cubic magnonic structures a lattice constant greater than the exchange length in the matrix material implies increased importance of dipolar interactions and thus results in an effective reduction of the gap width.

Finally, let us try to find the physical grounds of the presence of magnonic gaps resulting from the assumptions made in our model. Let us get back for a moment to Eq. (3) to ponder over the properties of the exchange field defined by this formula, an equivalent form of which is

$$\vec{H}_{\mathrm{ex}}(\vec{r}) = \lambda_{\mathrm{ex}}^2 \nabla^2 \vec{m} + (\nabla \lambda_{\mathrm{ex}}^2) \cdot (\nabla \vec{m}) + \lambda_{\mathrm{ex}}^2 \nabla^2 \vec{M}_S + (\nabla \lambda_{\mathrm{ex}}^2) \cdot (\nabla \vec{M}_S). \tag{28}$$

The effect of the nonhomogeneity of the magnetic structure on the exchange field is included in the last three terms in Eq. (28). Getting back to formula (11), which describes the space dependence of the spontaneous magnetization and the exchange length in the considered magnonic system, let us include them in the formula (28) for the exchange field. We get

$$\vec{H}_{\mathrm{ex}}(\vec{r}) = \begin{bmatrix} H_{\mathrm{ex}}^x \\ H_{\mathrm{ex}}^y \\ H_{\mathrm{ex}}^z \end{bmatrix} = \begin{bmatrix} \lambda_{\mathrm{ex}}^2 \nabla^2 m_x(\vec{r}) + \Delta\lambda_{\mathrm{ex}}^2 (\nabla S(\vec{r})) \cdot (\nabla m_x(\vec{r})) \\ \lambda_{\mathrm{ex}}^2 \nabla^2 m_y(\vec{r}) + \Delta\lambda_{\mathrm{ex}}^2 (\nabla S(\vec{r})) \cdot (\nabla m_y(\vec{r})) \\ \lambda_{\mathrm{ex}}^2 \Delta M_S \nabla^2 S(\vec{r}) + \Delta\lambda_{\mathrm{ex}}^2 \Delta M_S (\nabla S(\vec{r})) \cdot (\nabla S(\vec{r})) \end{bmatrix}, \tag{29}$$

where $\Delta M_S = M_{S,A} - M_{S,B}$ and $\Delta\lambda_{\mathrm{ex}}^2 = \lambda_{\mathrm{ex},A}^2 - \lambda_{\mathrm{ex},B}^2$. In the case of homogeneous material only the first terms in the expressions for components H_{ex}^x and H_{ex}^y are nonzero, and thus all the other terms describe the effect of the magnetic nonhomogeneity of the composite material. In an MC $S(\vec{r})$ is a periodic function with a unit step on the scattering center surface. In a structure consisting of spheres (of material A) of radius R embedded in a matrix (of material B) and forming a crystallographic lattice with lattice vectors $\vec{a}$, $S(\vec{r})$ can be written in the following form:

$$S(\vec{r}) = \sum_{\vec{a}} \theta(R - |\vec{r} - \vec{a}|), \tag{30}$$

where $\theta(x)$ is a Heaviside step function taking on value 1 when $x > 0$ and 0 otherwise. The nabla operator acting on this function produces the Dirac delta, $\nabla\theta(r) = \delta(0)$, localized at the interface between materials A and B. Thus, for the z component of the exchange field (29) we get

$$H_{\mathrm{ex}}^{z}(\vec{r}) = \Delta M_S \sum_{\vec{a}} [\lambda_{ex}^2 \nabla \delta(R - |\vec{r} - \vec{a}|) + \Delta\lambda_{\mathrm{ex}}^2 \delta^2(R - |\vec{r} - \vec{a}|)]. \tag{31}$$

The above expression suggests that the spatial structure of the field $H_{\mathrm{ex}}^{z}(\vec{r})$ consists of periodically distributed Dirac deltas, which can be regarded as the magnetic counterpart of the Kronig-Penney model.[141] It is exactly this analogy that provides a basis for explanation of the existence of magnonic gaps in the energy spectra of the magnetic systems considered in this study.

ACKNOWLEDGMENTS

The present study is financed from the Funds for Scientific Research granted for years 2007–2010 within the Research Project No. N N202 1945 33. The calculations presented in this study were performed in Poznań Supercomputing and Networking Center.

[1] D. R. Smith, W. J. Padilla, D. C. Vier, S. C. Nemat-Nasser, and S. Schultz, Phys. Rev. Lett. **84**, 4184 (2000).
[2] S. A. Ramakrishna, Rep. Prog. Phys. **68**, 449 (2005).
[3] A. Berrier, M. Mulot, M. Swillo, M. Qiu, L. Thylén, A. Talneau, and S. Anand, Phys. Rev. Lett. **93**, 073902 (2004).
[4] R. W. Ziolkowski, Phys. Rev. E **70**, 046608 (2004).
[5] M. Silveirinha and N. Engheta, Phys. Rev. Lett. **97**, 157403 (2006).
[6] M. F. Yanik and S. Fan, Phys. Rev. Lett. **92**, 083901 (2004).
[7] M. F. Yanik and S. Fan, Phys. Rev. A **71**, 013803 (2005).
[8] T. Baba and D. Mori, J. Phys. D **40**, 2659 (2007).
[9] L. Feng, X. P. Liu, M. H. Lu, Y. B. Chen, Y. F. Chen, Y. W. Mao, J. Zi, Y. Y. Zhu, S. N. Zhu, and N. B. Ming, Phys. Rev. Lett. **96**, 014301 (2006).
[10] L. Feng, X. P. Liu, M. H. Lu, Y. B. Chen, Y. F. Chen, Y. W. Mao, J. Zi, Y. Y. Zhu, S. N. Zhu, and N. B. Ming, Phys. Rev. B **73**, 193101 (2006).
[11] J. Li, Z. Liu, and C. Qiu, Phys. Rev. B **73**, 054302 (2006).
[12] M. Ambati, N. Fang, C. Sun, and X. Zhang, Phys. Rev. B **75**, 195447 (2007).
[13] G. Bertotti, C. Serpico, I. D. Mayergoyz, A. Magni, M. d'Aquino, and R. Bonin, Phys. Rev. Lett. **94**, 127206 (2005).
[14] T. Kimura, Y. Otani, and J. Hamrle, Phys. Rev. Lett. **96**, 037201 (2006).
[15] G. Finocchio, M. Carpentieri, B. Azzerboni, L. Torres, E. Martinez, and L. Lopez-Diaz, J. Appl. Phys. **99**, 08G522 (2006).
[16] B. Wang, Jian Wang, Jin Wang, and D. Y. Xing, Phys. Rev. B **69**, 174403 (2004).
[17] P. Bruno and V. K. Dugaev, Phys. Rev. B **72**, 241302(R) (2005).
[18] C. Herring and C. Kittel, Phys. Rev. **81**, 869 (1951).
[19] *Linear and Nonlinear Spin Waves in Magnetic Films and Superlattices*, edited by M. G. Cottam (World Scientific, Singapore, 1994).
[20] H. Puszkarski, Prog. Surf. Sci. **9**, 191 (1971).
[21] H. Puszkarski, Surf. Sci. Rep. **20**, 45 (1994).
[22] A. Aharoni, *Introduction to the Theory of Ferromagnetism*, 2nd ed. (Oxford University Press, Oxford, 2000).
[23] E. O. Kamenetskii, R. Shavit, and M. Sigalov, J. Appl. Phys. **95**, 6986 (2004).
[24] H. Puszkarski, M. Krawczyk, and J.-C. S. Lévy, J. Appl. Phys. **101**, 024326 (2007).
[25] In both cases, however, the retardation effects are assumed as negligible throughout this paper.
[26] C. L. Dennis *et al.*, J. Phys.: Condens. Matter **14**, R1175 (2002).
[27] M. J. Pechan, C. Yu, R. L. Compton, J. P. Park, and P. A. Crowell, J. Appl. Phys. **97**, 10J903 (2005).
[28] L. J. Heyderman *et al.*, Phys. Rev. B **73**, 214429 (2006).
[29] P. Politi and M. G. Pini, Phys. Rev. B **66**, 214414 (2002).
[30] J. Wang, A. O. Adeyeye, and N. Singh, Appl. Phys. Lett. **87**, 262508 (2005).
[31] E. Y. Tsymbal, Appl. Phys. Lett. **77**, 2740 (2000).
[32] M. Beleggia and M. De Graef, J. Magn. Magn. Mater. **285**, L1 (2005).
[33] S. A. Majetich and M. Sachan, J. Phys. D **39**, R407 (2006).
[34] M. Beleggia, S. Tandon, Y. Zhu, and M. De Graef, J. Magn. Magn. Mater. **278**, 270 (2004).
[35] N. Mikuszeit, E. V. Vedmedenko, and H. P. Oepen, J. Phys.: Condens. Matter **16**, 9037 (2004).
[36] K. L. Metlov, Phys. Rev. Lett. **97**, 127205 (2006).
[37] P. Vavassori, D. Bisero, F. Carace, A. di Bona, G. C. Gazzadi, M. Liberati, and S. Valeri, Phys. Rev. B **72**, 054405 (2005).
[38] G. N. Kakazei, Y. G. Pogorelov, M. D. Costa, T. Mewes, P. E. Wigen, P. C. Hammel, V. O. Golub, T. Okuno, and V. Novosad, Phys. Rev. B **74**, 060406(R) (2006).
[39] M. Demand, A. Encinas-Oropesa, S. Kenane, U. Ebels, I. Huynen, and L. Piraux, J. Magn. Magn. Mater. **249**, 228 (2002).
[40] S. Khizroev, Y. Hijazi, N. Amos, R. Chomko, and D. Litvinov, J. Appl. Phys. **100**, 063907 (2006).
[41] G. Gubbiotti, M. Madami, S. Tacchi, G. Carlotti, and T. Okuno, J. Appl. Phys. **99**, 08C701 (2006).
[42] G. Gubbiotti, S. Tacchi, G. Carlotti, N. Singh, S. Goolaup, A. O. Adeyeye, and M. Kostylev, Appl. Phys. Lett. **90**, 092503 (2007).
[43] Yu. V. Gulyaev and S. A. Nikitov, Dokl. Phys. **46**, 687 (2001).
[44] D. S. Deng, X. F. Jin, and R. Tao, Phys. Rev. B **66**, 104435 (2002).
[45] V. V. Kruglyak and A. N. Kuchko, Physica B **339**, 130 (2003).
[46] M. G. Cottam and D. R. Tilley, *Introduction to Surface and Superlettice Excitations* (Institute of Physics, Bristol, 2005).
[47] E. L. Albuquerque and M. G. Cottam, Phys. Rev. B **46**, 14543 (1992).
[48] S. H. Charap and J. O. Artman, J. Appl. Phys. **49**, 1585 (1978).
[49] N. Vukadinovic, O. Vacus, M. Labrune, O. Acher, and D. Pain, Phys. Rev. Lett. **85**, 2817 (2000).
[50] N. Vukadinovic, M. Labrune, J. Ben Youssef, A. Marty, J. C. Toussaint, and H. Le Gall, Phys. Rev. B **65**, 054403 (2001).
[51] C. Yu, M. J. Pechan, D. Carr, and C. J. Palmstrøm, J. Appl. Phys. **99**, 08J109 (2006).
[52] U. Ebels, L. Buda, K. Ounadjela, and P. E. Wigen, Phys. Rev. B **63**, 174437 (2001).

[53] N. Vukadinovic, M. Labrune, and J. Ben Youssef, Eur. Phys. J. B **50**, 593 (2006).
[54] H. Al-Wahsh, Phys. Rev. B **69**, 012405 (2004).
[55] A. Mir, H. Al Wahsh, A. Akjouj, B. Djafari-Rouhani, L. Dobrzynski, and J. O. Vasseur, J. Phys.: Condens. Matter **14**, 637 (2002).
[56] J. O. Vasseur, A. Akjouj, L. Dobrzynski, B. Djafari-Rouhani, and E. H. El Boudouti, Surf. Sci. Rep. **54**, 1 (2004).
[57] J. O. Vasseur, L. Dobrzynski, B. Djafari-Rouhani, and H. Puszkarski, Phys. Rev. B **54**, 1043 (1996).
[58] M. Krawczyk and H. Puszkarski, Acta Phys. Pol. A **93**, 805 (1998).
[59] M. Krawczyk and H. Puszkarski, Acta Physicae Superficierum **III**, 89 (1999).
[60] H. Puszkarski and M. Krawczyk, Solid State Phenom. **94**, 125 (2003).
[61] Yu. V. Gulyaev, S. A. Nikitov, L. V. Zhivotovskii, A. A. Klimov, Ph. Tailhades, L. Presmanes, C. Bonningue, C. S. Tsai, S. L. Vysotskii, and Yu. A. Filimonov, JETP Lett. **77**, 567 (2003).
[62] A. V. Butko, S. A. Nikitov, and Yu. A. Filimonov, J. Commun. Technol. Electron. **50**, 88 (2005).
[63] A. V. Butko, A. A. Klimov, S. A. Nikitov, and Yu. A. Filimonov, J. Commun. Technol. Electron. **51**, 944 (2006).
[64] S. L. Vysotskii, S. A. Nikitov, and Yu. A. Filimonov, JETP **101**, 547 (2005).
[65] L. Torres, L. Lopez-Diaz, O. Alejos, and J. Iniguez, Physica B **275**, 59 (2000).
[66] C. C. Wang, A. O. Adeyeye, and Y. H. Wu, J. Appl. Phys. **94**, 6644 (2003).
[67] L. J. Heyderman, H. H. Solak, F. Nolting, and C. Quitmann, J. Appl. Phys. **95**, 6651 (2004).
[68] C. Yu, M. J. Pechan, W. A. Burgei, and G. J. Mankey, J. Appl. Phys. **95**, 6648 (2004).
[69] S. McPhail, C. M. Gürtler, J. M. Shilton, N. J. Curson, and J. A. C. Bland, Phys. Rev. B **72**, 094414 (2005).
[70] S. A. Nikitov, Yu. A. Filimonov, and Ph. Tailhades, Adv. Sci. Technol. (Faenza, Italy) **45**, 1355 (2006).
[71] I. L. Lyubchanskii, N. N. Dadoenkova, M. I. Lyubchanskii, E. A. Shapovalov, and Th. Rasing, J. Phys. D **36**, R277 (2003).
[72] M. Inoue *et al.*, J. Phys. D **39**, R151 (2006).
[73] A. Figotin and I. Vitebsky, Phys. Rev. E **63**, 066609 (2001).
[74] A. Figotin and I. Vitebskiy, Phys. Rev. B **67**, 165210 (2003).
[75] A. M. Merzlikin, A. P. Vinogradov, M. Inoue, and A. B. Granovsky, Phys. Rev. E **72**, 046603 (2005).
[76] P. Xu and Z.-Y. Li, Phys. Lett. A **335**, 512 (2005).
[77] A. Saib, D. Vanhoenacker-Janvier, I. Huynen, A. Encinas, L. Piraux, E. Ferain, and R. Legras, Appl. Phys. Lett. **83**, 2378 (2003).
[78] A. Saib and I. Huynen, Electromagnetics **26**, 261 (2006).
[79] Y. Ikezawa, K. Nishimura, H. Uchida, and M. Inoue, J. Magn. Magn. Mater. **272**, 1690 (2004).
[80] S. A. Nikitov and Ph. Tailhades, Opt. Commun. **199**, 389 (2001).
[81] C. G. Sykes, J. D. Adam, and J. H. Collins, Appl. Phys. Lett. **29**, 388 (1976).
[82] Y. V. Gulyaev, S. A. Nikitov, and A. I. Volkov, J. Commun. Technol. Electron. **50**, 1024 (2005).
[83] E. Istrate and E. H. Sargent, Rev. Mod. Phys. **78**, 455 (2007).
[84] V. S. Tkachenko, V. V. Kruglyak, and A. N. Kuchko, J. Magn. Magn. Mater. **307**, 48 (2006).
[85] V. A. Ignatchenko, Yu. I. Mankov, and A. A. Maradudin, Phys. Rev. B **62**, 2181 (2000).
[86] V. V. Kruglyak and A. N. Kuchko, Phys. Met. Metallogr. **93**, 511 (2002).
[87] J. F. Galisteo, F. Garcia-Santamaria, D. Golmayo, B. H. Juárez, C. López, and E. Palacios, J. Opt. A, Pure Appl. Opt. **7**, S244 (2005).
[88] C. Lopez, J. Opt. A, Pure Appl. Opt. **8**, R1 (2006).
[89] S. G. Reidy, L. Cheng, and W. E. Bailey, Appl. Phys. Lett. **82**, 1254 (2003).
[90] J. Fassbender and J. McCord, Appl. Phys. Lett. **88**, 252501 (2006).
[91] J. Melngailis, J. Vac. Sci. Technol. B **5**, 469 (1987).
[92] J. Fassbender *et al.*, Appl. Phys. A: Mater. Sci. Process. **77**, 51 (2003).
[93] J. McCord, T. Gemming, L. Schultz, J. Fassbender, M. O. Liedke, M. Frommberger, and E. Quandt, Appl. Phys. Lett. **86**, 162502 (2005).
[94] V. Dasgupta, N. Litombe, W. E. Bailey, and H. Bakhru, J. Appl. Phys. **99**, 08G312 (2006).
[95] J. Fassbender, D. Ravelosona, and Y. Samson, J. Phys. D **37**, R179 (2004).
[96] J. H. Kim, J. Kim, S. U. Lim, C. K. Kim, C. S. Yoon, G. J. Lee, and Y. P. Lee, J. Appl. Phys. **99**, 08G311 (2006).
[97] M. J. Pechan, C. Yu, D. Owen, J. Katine, L. Folks, and M. Carey, J. Appl. Phys. **99**, 08C702 (2006).
[98] K. Nielsh, R. B. Wehrspohn, J. Barthel, J. Kirschner, U. Gösele, S. Fischer, and H. Kronmüller, Appl. Phys. Lett. **79**, 1360 (2001).
[99] Y. Ikezawa, K. Nishimura, H. Uchida, and M. Inoue, J. Magn. Magn. Mater. **272**, 1690 (2004).
[100] J. Y. Cheng, W. Jung, and C. A. Ross, Phys. Rev. B **70**, 064417 (2004).
[101] C. A. Ross *et al.*, Phys. Rev. B **65**, 144417 (2002).
[102] C. A. Ross *et al.*, J. Appl. Phys. **91**, 6848 (2002).
[103] D. B. Terris and T. Thomson, J. Phys. D **38**, R199 (2005).
[104] J. I. Martiń, J. Nogu'es, K. Liu, J. L. Vicent, and I. K. Schuller, J. Magn. Magn. Mater. **256**, 449 (2003).
[105] M. Sachan, N. D. Walrath, S. A. Majetich, K. Krycka, and Chi-Chang Kao, J. Appl. Phys. **99**, 08C302 (2006).
[106] D. Farrell, Y. Ding, S. A. Majetich, C. Sanchez-Hanke, and C. C. Kao, J. Appl. Phys. **95**, 6636 (2004).
[107] S. Sun and C. B. Murray, J. Appl. Phys. **85**, 4325 (1999).
[108] S. Sun, C. B. Murray, D. Weller, L. Folks, and A. Moser, Science **287**, 1989 (2000).
[109] G. A. Melkov, V. I. Vasyuchka, A. V. Chumak, V. S. Tiberkevich, and A. N. Slavin, J. Appl. Phys. **99**, 08P513 (2006).
[110] S. Choi, K.-S. Lee, and S.-K. Kim, Appl. Phys. Lett. **89**, 062501 (2006).
[111] J. Podbielski, F. Giesen, and D. Grundler, Phys. Rev. Lett. **96**, 167207 (2006).
[112] S. V. Vasiliev, V. V. Kruglyak, M. L. Sokolovskii, and A. N. Kuchko, J. Appl. Phys. **101**, 113919 (2007).
[113] R. Hertel, W. Wulfhekel, and J. Kirschner, Phys. Rev. Lett. **93**, 257202 (2004).
[114] D. D. Stancil, Progress In Electromagnetic Research Symposium 2005, Hangzhou, 23–26 August 2005 (unpublished).
[115] M. Bauer, C. Mathieu, S. O. Demokritov, B. Hillebrands, P. A. Kolodin, S. Sure, H. Dotsch, V. Grimalsky, Y. Rapoport, and A. N. Slavin, Phys. Rev. B **56**, R8483 (1997).
[116] V. Veerakumar and R. E. Camley, Phys. Rev. B **74**, 214401 (2006).

[117] A. K. Zwezdin and V. I. Belotelov, Eur. Phys. J. B **37**, 479 (2004).
[118] H. Puszkarski, M. Krawczyk, J.-C. S. Lévy, and D. Mercier, Acta Phys. Pol. A **100**, 195 (2001).
[119] S. A. Nikitov, Ph. Tailhades, and C. S. Tsai, J. Magn. Magn. Mater. **236**, 320 (2001).
[120] L. Dobrzynski, B. Djafari-Rouhani, and H. Puszkarski, Phys. Rev. B **33**, 3251 (1986).
[121] C. Bayer, M. P. Kostylew, and B. Hillebrands, Appl. Phys. Lett. **88**, 112504 (2006).
[122] M. P. Kostylev, A. A. Stashkevich, and N. A. Sergeeva, Phys. Rev. B **69**, 064408 (2004).
[123] V. V. Kruglyak, R. J. Hicken, A. N. Kuchko, and V. Yu. Gorobets, J. Appl. Phys. **98**, 014304 (2005).
[124] R. Qiu, Z. Zhang, L. Guo, C. Ying, and J. Liang, Phys. Status Solidi B **243**, 1983 (2006).
[125] M. Shamonin, A. Snarskii, and M. Zhenirovskyy, NDT & E Int. **34**, 35 (2004).
[126] L. Giovannini, F. Montoncello, and F. Nizzoli, Phys. Rev. B **75**, 024416 (2007).
[127] R. Arias and D. L. Mills, Phys. Rev. B **63**, 134439 (2001).
[128] R. Arias and D. L. Mills, Phys. Rev. B **70**, 094414 (2004).
[129] P. Chu, D. L. Mills, and R. Arias, Phys. Rev. B **73**, 094405 (2006).
[130] V. V. Krugkyak and A. N. Kuchko, Phys. Met. Metallogr. **92**, 211 (2001).
[131] V. V. Krugkyak and A. N. Kuchko, J. Magn. Magn. Mater. **272-276**, 302 (2004).
[132] J. Dubowik, Phys. Rev. B **54**, 1088 (1996).
[133] R. Skomski, G. C. Hadjipanayis, and D. J. Sellmyer, IEEE Trans. Magn. **43**, 2956 (2007).
[134] J. D. Joannopoulos, R. D. Meade, and J. N. Winn, *Photonic Crystals: Molding the Flow of Light* (Princeton University, Princeton, NJ, 1995).
[135] J. W. Haus, H. S. Sozuer, and R. Inguva, J. Mod. Opt. **39**, 1991 (1992).
[136] We have also performed convergence tests for MCs consisting of ferromagnetic scattering centers embedded in a nonmagnetic matrix, as well as for antiparallel alignment of magnetic moments in the centers and in the matrix. However, in both cases, besides imaginary eigenvalues, we obtained real eigenvalues corresponding to imaginary spin-wave frequencies and showing no convergence improvement with increasing number of vectors $\vec{G}$. Hence, the equations derived in this paper only apply to MCs composed of two ferromagnetic materials with parallel alignment of the magnetization vectors.
[137] M. Krawczyk and H. Puszkarski, Cryst. Res. Technol. **41**, 547 (2006).
[138] V. V. Kruglyak and R. J. Hicken, J. Magn. Magn. Mater. **306**, 191 (2006).
[139] R. P. Cowburn, J. Phys. D **33**, R1 (2000).
[140] M. Krawczyk and H. Puszkarski, J. Appl. Phys. **100**, 073905 (2006).
[141] R. de L. Kronig and W. G. Penney, Proc. R. Soc. London, Ser. A **130**, 499 (1931).